Available online at www.elixirpublishers.com (Elixir International Journal)

Crystal Research Technology

Elixir Crystal Research Tech. 116 (2018) 50159-50163

ISSN: 2229-712X

Electrical Studies on Al Substituted ZnMg Mixed Ferrite Prepared by Sol-Gel Method

Ramesh C[1], K.Maniysundar[2],Selvanandan.S[2,*] and Anandhi.D.V[2]

[1]Sathyabama University, Chennai, India

[2]ACS College of Engineering, Bangalore, Karnataka, India.

ARTICLE INFO

Article history:

Received: 16 February 2018;

Received in revised form:

5 March 2018;

Accepted: 15 March 2018;

Keywords

Sol-gel method,

XRD,

SEM.

ABSTRACT

Al-substituted ZnMg mixed ferrite prepared by conventional sol-gel method. Al substituted ZnMg ferrite of molecular formula $Zn_{0.7}Mg_{0.3}Al_xFe_{2-x}O_4$ & $Zn_{0.5}Mg_{0.5}Al_xFe_{2-x}O_4$ where (x=0.0, 0.1, 0.2, 0.3, 0.4) were prepared. The obtained samples were sintered at 850^0C for 4 hours. The XRD used to study the structural properties such as particle size, lattices constant and the effect of doping concentration of Al atoms is discussed. The Structural images from XRD, SEM were presented. The Electrical characteristics of these mixed ferrites were studied using Cyclic Voltometric Analysis to measure logarithm of conductivity (log σ), dielectric constant (ϵ) and loss factor at various frequencies and are reported. Hopping of electrons between localized stated of cations in the interstitial sites were discussed. The variation of activation energy with various ranges of frequencies was reported.

Introduction

Ferrites are magnetic semiconductors with high resistivity. These materials are used as inductor, cores of transformers, recording heads, antenna rods, microwave devices and henceforth[1-4]. The process of ferrite materials play a vital role in various specific applications to achieve better magnetic properties[5]. There are several methods of preparation of ferrite including sol-gel[6], co-precipitation[7], hydrothermal[8], high energy ball milling[9] and micro emulsion[10] are developed to make fine structured ferrite. Among these methods, the citrate sol-gel method has unique advantage over other one for the preparation of nanosized ferrite compounds.

Substitution of Al for Fe can occupy various positions on the tetrahedral [A] and octahedral [B] sites and changes the microstructure, electric and magnetic properties of the compound. Hence, the different properties can be obtained to suit for a specific applications[11]. Recently, diamagnetic substitution in mixed ferrite has received special attention in modifying the physical properties of basic ferrites which are the promising materials for high quality, low cost, low loss at high frequency for power application. These materials are in high demand in electronic industry. H.Mohseni.et.al., studies Mn doped Mg-Zn ferrite particle. Cation site preferences have caused a large variation in the magnetic ions concentration over the two sub-lattices giving rise to significant change in the strength of sub-lattice magnetic moment[12]. M.A.Gabal.et.al., the structural, electrical and magnetic properties were studied on Al substitution on MnZn ferrite nanopowders. The substitution of Fe^{3+} ions by diamagnetic Al^{3+} ions, which have strong preference for occupying the octahedral[B] sites decreases the magnetic moment and consequently the net magnetization through weakening of A-B interactions and disturbing the spin ordering[13]. The Al^{3+} ions have a tendency to occupy both A and B site, the replacement of Fe^{3+}, each having a magnetic moment of $5\mu_B$ was reported by V.K.Babbar et.al., in his study on Ni-Sn-Al ferrites for high frequency applications[14].

The increase of M_s upon Al substitution of 0.015 may due to decrease in canting angle (α_{YK}) between moments in B site due to decrease of the negative B-B interactions was presented by Hamed Baheraei.et.al[15]. Al^{3+} strongly preferred to occupy the octahedral site for Fe^{3+}, decreases the magnetic moment of octahedral site was reported by M.Mozaffari.et.al[16]. various other authors like M.A.Ahmed et.al., Ali.A.Atiet.et.al., K.Raju et.al., discussed about site preference of occupancy of Al^{3+} ions in A & B site[17,18,19]. The increase in coercive force of Mg-Al ferrite with increase of Al_2O_3 concentration primarily due to an increase in the concentration of second phase inclusion was reported by V.F.Belov et.al.,[20] FTIR studies on Al substituted MnZn mixed ferrite was studied by Chandrasekaran et.al. Higher concentration of Al induces local distortion on the exchange of charge carriers, which alter the band gap of localized ‘d’ band[21]. In this paper, the Al substituted ZnMg mixed ferrites of $Zn_{0.7}Mg_{0.3Alx}Fe_{2-x}O_4$ & $Zn_{0.5}Mg_{0.5Alx}Fe_{2-x}O_4$ $Mg_{0.5}Zn_{0.5}Al_xFe_{(2-x)}O_4$ where (x=0.0, 0.1, 0.2, 0.3, 0.4) synthesized by sol-gel method. The effect of doping concentration on structural and Electrical properties of as prepared samples was discussed in detail.

2. Experimental

$Zn_{0.7}Mg_{0.3}Al_xFe_{2-x}O_4$ & $Zn_{0.5}Mg_{0.5}Al_xFe_{2-x}O_4$ where (x=0.0, 0.1, 0.2, 0.3, 0.4) of analytical grade magnesium nitrate, zinc nitrate, aluminum nitrate and ferric nitrate were taken according to the stoichiometric ratio and dissolved in

Tele:

E-mail address: selvanandan@gmail.com

distilled water to obtain a mixed solution. Reaction procedures were carried out in air atmosphere. Ammonia solution was slowly added to maintain pH of 7. The pH value of the mixed solutions was measured by using a PHS-29A meter. Resulting solution were kept in hot plate with continuous stirring and heating at about 150^0 C until it becomes brown gel. The resulting gel was kept for double sintering at 850^0 C and 1100^0 C successively. The fine powders were obtained by grinding the sample using piston and mortar with acetone as a binder. X-ray diffraction (XRD) pattern of these ferrite powders were measured using a Rigaku D/Max 2400 X-ray diffractometer with Cu K_α radiation (40kV, 30 mA), the scanning electron micrographs were obtained on Scanning Electron Microscope **(**FEI Quanta FEG 200**)** and Cyclic Voltametric analysis used to determine the dielectric constant, impedance and loss factor.

CV or cyclic voltammetry is one of the potentiodynamic type used for electrochemical measurement. In the CV experiment, the potential of working electrode is ramped versus time in linearly. It is not like linear sweep voltammetry, the potential of working electrode potential is ramped in the opposite direction to return to the initial potential in CV experiment. Those ramp cycles in potential may be repeated as oftentimes as preferred. To present the cyclic voltammogram outline, the obtained working electrode current is plotted against the voltage we applied (i.e., potential of working electrode). Generally, CV is utilized to revise the electrochemical study of an unknown analyte in the electrolytic solution. The Schematic representation of cyclic voltammetry analysis is shown in figure 1.

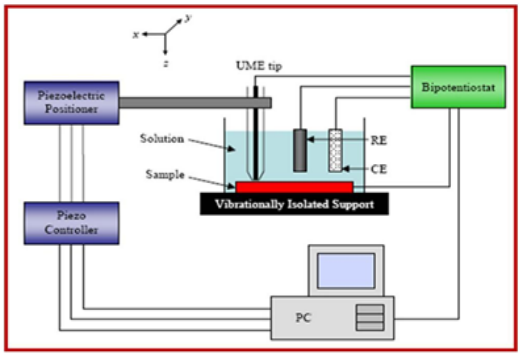

Figure 1. Schematic representation of cyclic voltammetry analysis.

The cell consists of electrodes to be fitted, the solvent in the solution, in which the species and dissolved electrolyte going to be studied using CV experiment. A well-known CV experiment make use of a cell outfitted with three electrode system figure 2: a reference electrode, working electrode, and the counter electrode. This aggregate is every so often called a 3-electrode arrangement. The electrolyte is generally brought to the sample solution to make sure conductivity become adequate. In the working electrode, material composition, electrolyte and solvent are going to determine the range of potential that may be accessed at some point of the experimentation. usual working electrode is deficient in running the cyclic voltammetry experiments, peak current and resistance going to be high in the high scan rate, which result in distortions. The current and resistance can be limited by using ultra microelectrodes. The counter electrode is also called as the auxiliary electrode, it will not react with the electrolytic solution and may be any material that conducts current without difficulty. Reactions going on at the surface of the counter electrode are insignificant as extended because it persists in conducting current properly. The counter electrode will frequently oxidize or reduce the solvent or bulk electrolyte is necessary to hold the observed current. The variety of electrolytes is greater restricted in non-aqueous solvents and a well-liked option is tetra butyl ammonium hexafluorophosphate ("TBAF").

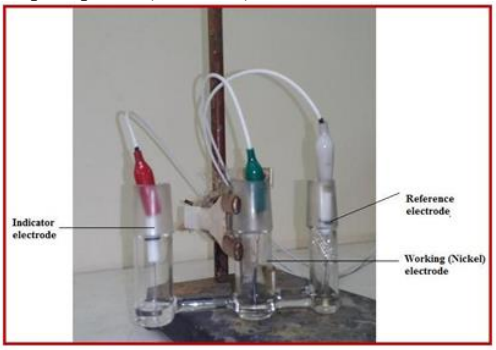

Figure 2. Cyclic voltammetry tri-electrode chamber.

3. Results and Discussion

3.1 Structural studies

The X-Ray diffraction pattern of the sample $Zn_{05}Mg_{0.5}Al_xFe_{2-x}O_4$ and $Zn_{0.7}Mg_{0.3}Al_xFe_{2-x}O_4$ and (x=0.0, 0.1, 0.2, 0.3, 0.4) are shown in Figure. 3 (a) & (b). The reflections from the planes (111), (311), (400) and (411) are predominantly found in all the samples. This indicates the spinel cubic structure. There are some additional peaks near (311) are seen when Al^{3+} was substituted and the peaks subsequently reduced in increase of Al^{3+}. It is believed that the Al^{3+} content induces lattice distortion and redistribution of Al^{3+}, Fe^{3+} and Zn^{2+} happens in both tetrahedral (A site) and octahedral sites (B site). The lattice parameter 'a', average grain size 'd' and cell volume 'V' were calculated according to equation (1), (2) and (3)[21,22],

$$a = \sqrt{\frac{\lambda}{4\sin^2\theta}\left(h^2+k^2+l^2\right)} \quad (1)$$

$$d = \frac{0.9\lambda}{\beta\cos\theta} \quad (2)$$

$$\& V = a^3 \quad (3)$$

Where, λ is the wavelength of X-Ray radiation ($1.5406A^0$), 2θ is the diffraction angle, β is the full width and half maximum (FWHM) of diffraction peak and (h k l) are miller indices of the corresponding peak.

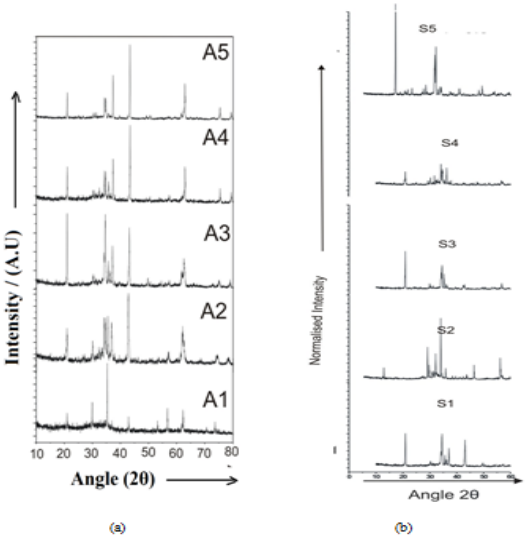

Figure 3 (a) & (b): XRD pattern of $Zn_{0.7}Mg_{0.3Alx}Fe_{2-x}O_4$ (x = 0.0:A1, x = 0.1:A2, x = 0.2:A3, x = 0.3:A4, x=0.4:A5.) & $Zn_{0.5}Mg_{0.5Alx}Fe_{2-x}O_4$ (x = 0.0:S1, x = 0.1:S2, x = 0.2:S3, x = 0.3:S4, x=0.4:S5.).

Moreover, from Figure. 5, with the Al^{3+} doping increases, there was a continuous decreases in lattice constant from $8.435A^0$ $8.362A^0$. while grain size decreases from 92nm to 26nm. The decreasing nature of lattice constant may due to replacement of smaller radii Fe^{3+}(r_{Fe} =0.67 A^0) since Al^{3+} preferentially occupy B site [21], the replacement continues as Al^{3+} substitution increases in our sample.

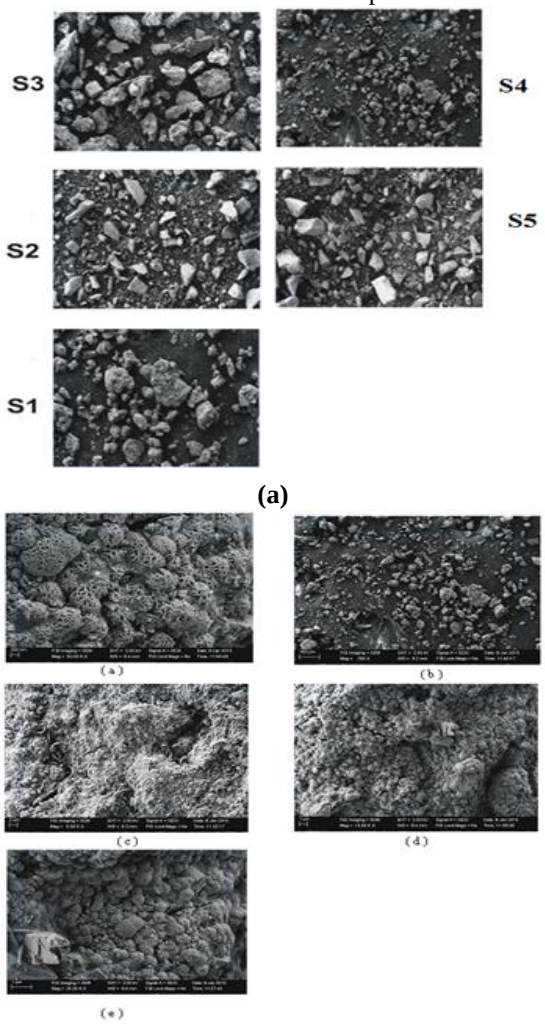

Figure 4 (a) & (b). SEM images $Zn_{0.7}Mg_{0.3Al_x}Fe_{2-x}O_4$ (x=0.0:a,x=0.1:b,x=0.2:c,x= 0.3:d,x=0.4:e.) & $Zn_{0.5}Mg_{0.5Al_x}Fe_{2-x}O_4$ (x=0.0:S1, x=0.1:S2, x = 0.2:S3, x = 0.3:S4, x=0.4:S5.).

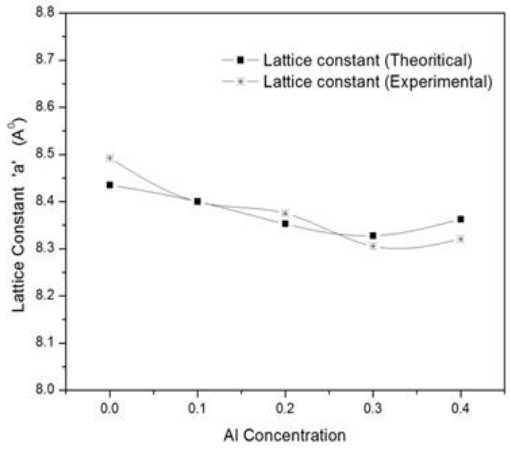

Figure 5. Variation of Lattice constant with Al concentration.

Figure 4(a) & (b) shows, the SEM images of Al^{3+} substituted MgZn mixed ferrite as function of Al^{3+} content. It can be observed that the grain size decreases with increase in Al substitution in these mixed ferrites. This may be due to the formation of aluminum oxides at given boundaries which inhibits the grain growth.

Table 1. Variation of Theoritical Lattice constant, Particle size and strain with Ni concentration in $Mg_{0.3}Zn_{0.7}Al_xFe_{2-x}O_4$ Ferrites.

Ni Concentration	Lattice constant 'a' (Å)	Particle Size (Å)	Strain	c/a Ratio	U-Parameter
0.0	8.4352	53.5	0.061	0.311	1.610
0.1	8.4003	92.6	0.055	0.326	1.607
0.2	8.3526	40.41	0.056	0.310	1.590
0.3	8.3277	32.1	0.041	0.322	1.602
0.4	8.3629	26.75	0.039	0.352	1.619

The average grain size varies from 90 nm to 20 nm for (x=0.0, 0.1, 0.2, 0.3, 0.4) respectively reported in Table 1. A comparative plot of particle size from XRD & SEM is shown in figure 6. The srain and U paramenter is represented in form of graph in figure 7.

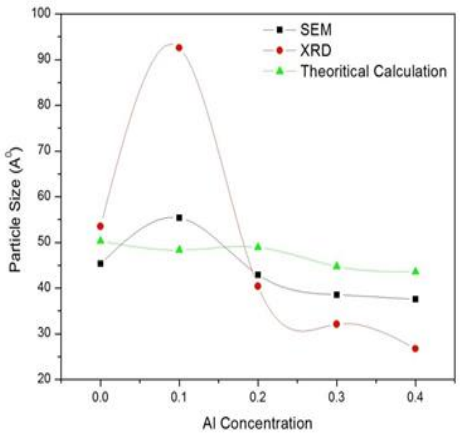

Figure 6. Variation of Particle Size with Al concentration

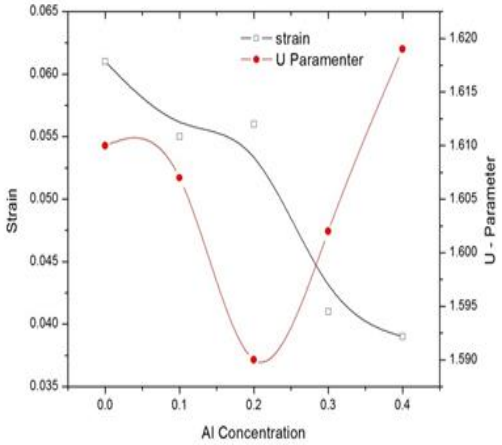

Figure 7. Change in Strain, U Parameter values with Al Concentration.

3.2 Electrical Properties

The dielectric behavior of a ferrite material has significant impact on sample synthesis technique, particle size, ion distribution etc., Figure 8 & 9 shows the frequency response curve with dielectric constant Z' at room temperature for $Zn_{0.7}Mg_{0.3}Al_xFe_{2-x}O_4$ & $Zn_{0.5}Mg_{0.5}Al_xFe_{2-x}O_4$ Ferrite system. Materials with high d.c. resistivity has less value of Z' and vice-versa[22]. In most of the ferrite the value of dielectric constant Z' decreases with increasing frequency. Polarisation mechanism which is very similar to that of

conduction mechanism in ferrite can be adopted to explain the dielectric nature in Zn ion substituted ferrite system.

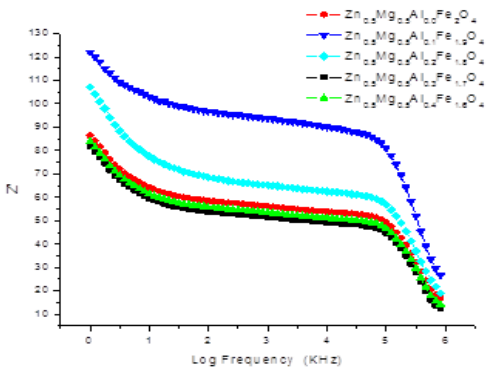

Figure 8. Plot of Z' Vs Log Frequency.

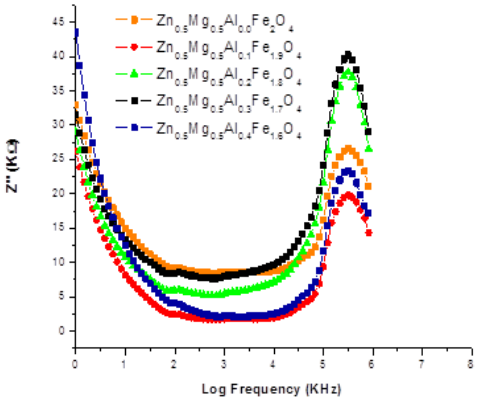

Figure 9. Plot of Z'' Vs Log Frequency.

The total polarisation in ferrite is mostly contributed by space charge polarization, led by total number of space charge carriers and conductivity in ferrites. And density of localized states liable for hopping of ions between A site and B site and end displacement of ions with respect to the applied electric field. The Zn substitution of ions increases Zn content in B site, inturn reduces the Fe content in B site. Ion is the prime material for both hopping exchange among localized states and space charge polarization. Therefore decrease in polarization is attributed mainly due to increase in Zn ions which is concluded by decrease of dielectric constant Z'.

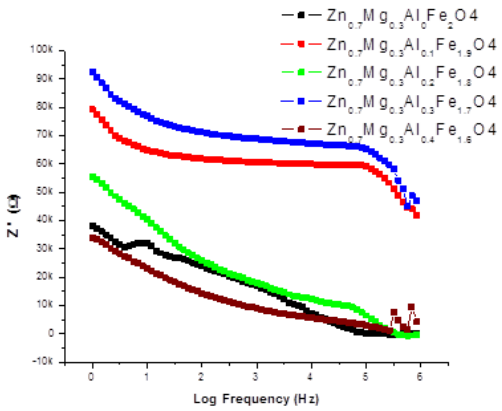

Figure 10. Plot of Z' Vs Log Frequency.

The grain boundary effect is predominant low frequency region[24]. The narrow in grain boundary the greater value in dielectric constant is. At higher frequency region the exchange interaction is not obey the Fe^{2+} and Fe^{3+} interactions in ferrite system with increase in frequency the dielectric content decreases from its higher value. The first curve in ferrite is due to dielectric ions. The plot of Z'' Vs Log frequency is shown in Figure 10 & 11. The behavior of dielectric loss is similar expect at higher frequencies. The smaller value of dielectric constant in ferrite is best suitable for higher frequency applications. The random raise in $Z^{''}$ in high frequency range from figure may be due to electronic exchange between Fe^{2+} and Fe^{3+} and the jumping frequencies of localized change cameras. The low dielectric parameters attributes to highly homogeneous and structured ferrites.

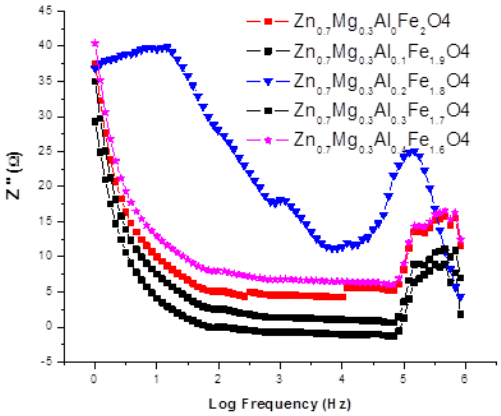

Figure 11. Plot of Z'' Vs Log Frequency.

The impedance spectroscopy is a helpful and effective experimental method that makes us to relate the material with its microstructure, i.e., grains, interfaces, grain boundaries of crystalline nano ferrites over a wide frequency range. A plot of Z'' Vs Z for $Zn_{0.7}Mg_{0.3}Al_xFe_{2-x}O_4$ & $Zn_{0.5}Mg_{0.5}Al_xFe_{2-x}O_4$ given in Figure (12 & 13). There is a probability of arc at high and low frequency region attribute to the share from grain boundaries in turn due to combined effect of gain boundary entrance and grain boundary capacitance. At high frequency semi circles are due to parallel combination of its resistance and capacitance.

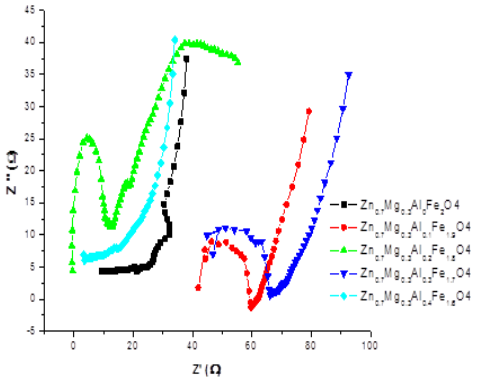

Figure 12. Plot of Z'' Vs Z'.

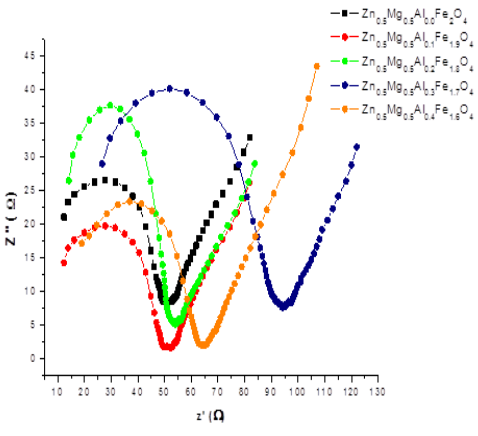

Figure 13. Plot of Z'' Vs Z'.

Nyquist Plot or Cole-Cole plot were plotted for a frequency range from 20 Hz to 50 MHz at room temperature. In N series sample almost all exhibit semi-circle at low frequency regains attribute to smaller grain size. The size of the semi-circle changes with the grain size and number of grains. The diameter of these semi circles is reprocative of this grain interior resistance. When we observe for S series samples x=0.2 and x=0.4 has semi-circle at low frequencies but are not completed at higher frequencies may due to the fact that grain boundary resistance and grain resistance are out of measurement region. The very low leakage current density of the order of 10^{-4} A/Cm^2 measured at field strength of 0.2 V/cm.

4. Conclusion

A series of $Zn_{0.7}Mg_{0.3}Al_xFe_{2-x}O_4$ & $Zn_{0.5}Mg_{0.5}Al_xFe_{2-x}O_4$ nanoferrite were prepared using sol-gel method. This spinel structure is confirmed by XRD analysis. The nano crystalline samples with grain size of 92 nm to 26 nm were obtained in which the lattice constant varies from 8.435 Å to 8.362 Å. The SEM measurement confirms the crystalline size with XRD data. Replacement of Al^{3+} on Fe^{3+} occupy octahedral site thus reduces A-B interaction intern reduces particle size. The trend in conductivity shows that mixed ferrite have more electrons for transport at high frequencies. The variation of dielectric constant Vs frequency is these materials is explained to be due to the effective value of polarization caused by interionic, particles and grain-boundary effect at low frequencies. The low value of dielectric constant at high frequencies is attributed to a lower contribution of polarisation due to exclusively to interionic type. It is explained thus because of the release of charge carriers from the effect of polarization in the high frequency region. The behavior of polarization with frequency can be explained using Koop's theory. i.e., Hopping of charge carriers between Fe^{2+} and Fe^{3+} ions are the main mechanism for electrical conduction.

5. References

[1] H. J. Ritcher, *J.Appl.Phys*.32(**1999**)R147.
[2] H. Gleiter, J. Weissmuller, O. Wollersheim, R. Wurschum, *Acta. Mater*. 49 (**2001**) 737.
[3] Alex. Goldman: Modern ferrite technology, Springer, New York, **2006**.
[4] B. G. Toksha, Sagar E. Shirsath, S. M. Patange, K. M. Hadhav, *Solid. State. Comm*. 147 (**2008**) 479.
[5] K. Haned, A. H. Morris, *J. Appl. Phys*. 63 (**1998**) 4258.
[6] P. P. Hankere, R. P. Patil, U. B. Sankpal, S. D. Jadhav, K. M. Garadhar, S. N. Achary, *J. Alloy and Comp*. 509 (**2011**) 276-280.
[7] C. F. Zhang, X. C. Zhong, H. Y. Yo, Z. W. Liu, D. C. Zeng, *Physica B: Cond. Matt*., 404 (**2009**) 2327-2331.
[8] L. Nalbandian, A. Delimitis, V. T. Zaspalis, E. A. Deliyanni, D. N. Bakoyannakis, E. N. Peleka, *Microporous and mesoporous mats.*114 (**2008**) 465-473.
[9] B. Gillot, B. Domenichini, *Mater. Chem. and Phys*.47 (**1994**) 217-224.
[10] D. S. Mathew, R. S. Juang, *Chemical Emgineering* J. 129 (**2007**) 51-65.
[11] C. Venkatarajua, Sathishkumar, K. Sivakumar, *J. Alloys. Compd*. 498 (**2010**) 203.
[12] H. Mohseni, H.Shokrollahi, Ibrahim Sharifi, Kh. Gheisari, *J. Magm and Mag. Mat.* 324 (**2012**) 3741-3447.
[13] M. A. Gabal, A. M. Abdel-Daiem, Y. M. Al Angari, I. M. Ismail, *Polyhedron*, 57(**2013**)105-111.
[14] V. K. Babbar, J. S. Chandel, S. P. Sud, *J. of Mat. Sci. Letts*. 14 (**1995**) 763-765.
[15] Hamed Bahiraei, Morteza Zargar Shoushtari, K. Gheisari, C. K. Ong, *J. Mag and Mag. Mat*. 371(**2014**) 29-34.
[16] M. Mozaffari, Z. Abooalizadeh, J. Amighian, *J. Mag. and Mag. Mat*., 323(**2011**)2997-3000.
[17] M. A. Ahmed, A. Tawfik, M. K. El-nimr, A. A. El-hasab, *J. of Mat. Sci.Lett*., 10 (**1991**) 549-551.
[18] Ali A. Ati, Zulkafli Othaman, Alireza Samavati, Fatemeh Yaghoubi Doust, *J. Mol. Stru*., 1058 (**2014**) 136-141.
[19] K. Raju, C. G. Balaji, P. Venugopal Reddy, *J. Mag. and Mag. Mat,* 354 (**2014**) 383-387.
[20] V. K. Belov, T. A. Khimich, M. N. Shipko, E. V. Korneev, L. M. Letyuk, Izves. Vyssh. Ucheb. Zaved.. Fizika, UDC 538.221 (**1971**) 105-109.
[21] G. Chandrasekaran, S. Selvanandan, K. Manivannane, *J.o f Mat. Sci. Mat. in Elec*.15 (**2004**) 15-18.
[22]Amarendra Singh K, Goel T C, Mendiratta R G, Thakur O P and Chandra Prakash 2002 *J. Appl. Phys.* 91 6626
[23]C. G. Koops, On the dispersion of resistivity and dielectric constant of some semiconductors at audio frequencies *Phy. Rev.*, 83 (1951) 121.